

# ENERGY-BASED METHOD FOR GAS TURBINE ENGINE DISK BURST SPEED CALCULATION

Anton N. Servetnik

Central Institute of Aviation Motors, Moscow, Russia

servetnik@ciam.ru

**Keywords:** spin disk testing, burst speed, fracture criterion, strain energy density

## Abstract

*FE modeling of burst speed tests of gas turbine engine (GTE) disks using stress-strain properties confirmed by tensile tests of specimen was carried out. Stress strain state (SSS) of disk during loading was determined using the MSC. Software and ANSYS commercial FE method software. Incremental theory of plasticity with isotropic hardening was used to determine the distribution of plastic strains of disks during loading. It was shown a strong sensitivity of the burst speed to the choice of the yield function. Burst speed test results of various disk configurations and thermo-mechanical loadings were compared with three-dimensional elastic-plastic FEM analysis results using energy-based fracture criteria.*

## Nomenclature

$\varepsilon_{ij}$  - strain tensor components  
 $\varepsilon^{pl}$  - plastic strain  
 $\sigma_{ij}$  - stress tensor components  
 $\sigma_1$  - first principal stress  
 $\sigma_2$  - second principal stress  
 $\sigma_3$  - third principal stress  
 $\sigma_\theta$  - engineering circumferential stress  
 $\sigma_r$  - engineering radial stress  
 $\sigma_B$  - ultimate strength  
 $\sigma_{eqv}$  - equivalent stress  
 $U$  - strain energy density  
 $U_{aver}$  - average strain energy density obtained at calculations made by average values of mechanical material properties  
 $U_{min}$  - minimal strain energy density obtained at calculations made by minimum values of mechanical material properties

$U^*$  - critical value of strain energy density

$U^*_{aver}$  - critical value of strain energy density obtained at average values of monotonic tensile tests

$U^*_{min}$  - critical value of strain energy density obtained at minimal values of monotonic tensile tests

$n_{100\%}$  - rotor speed at maximum engine regime

$n_{burst}$  - burst speed reduced to  $n_{100\%}$

$n_{KB}$  - burst margin

$\Delta R$  - radial elongation of disk

$R, r$  - radius

$r^*$  - radius of disk cylindrical section

## 1. Introduction

In recent years the GTE development and certification efforts actively have been engaging the calculations which have made it possible to assess a load-carrying capability of disk (burst speed) that is made from material having the most unfavorable mechanical properties instead of the experimental disk strength validation.

Many methods have been developed to assess the burst speed of disks. The limit equilibrium method is the traditional method to assess disk load-carrying capability during designing [1]. This method is based on the assumption that fracture occurs over meridian or cylindrical disk sections ( $r = r^*$ ) when:

$$\sigma_\theta(r) = \sigma_B(r), \quad (1)$$

$$\sigma_r(r^*) = \sigma_B(r^*). \quad (2)$$

The condition (1) means that circumferential stresses are equal to ultimate strength of

material in all the points of meridian disk section. The condition (2) means that radial stresses are equal to ultimate strength over cylindrical section at radius  $r^*$ . Criteria (1) and (2) should be used simultaneously. When determining the burst speed by this method, simple calculative schemes are used that don't take into account influence of stress concentration, 3D SSS, effect of mating parts and real thermal field of disk. The distinction between calculative values and experimental data comes to 20% in some cases.

Use of FEM in calculations makes it possible to take into account both structural and loading peculiarities and statistical scatter of material properties. While developing a technique to assess a load-carrying capability of disks, selection of material model and fracture criterion is of great importance. Verification technique is required to be made based on comparison of calculative data with experimental ones. The developed criterion must be checked for analysis of different disk designs made from various alloys. In this work the energy-based fracture criterion was selected as fracture criterion [2]. This criterion states that fracture occurs at the instant when strain energy density reaches its critical value  $U^*$  in the most stressed disk point:

$$U = U^* \tag{3}$$

Strain energy density at a point of arbitrary loaded elastic-plastic body is defined by formula:

$$U = \int_0^\varepsilon \sigma_{ij} d\varepsilon_{ij} , (i, j = 1, 2, 3), \tag{4}$$

Energy density value is the sum of two constituents  $U=U_0+U_f$ , where  $U_0$  corresponds to strain energy density of volume change with no change in form and  $U_f$  corresponds to strain energy density of form change with no change in volume.

In [3] and [4] it was shown a strong sensitivity of the burst speed to choice of the yield

function. Different yield surfaces with the use of Hosford model [5] have been investigated to find the best suited surface shape. In this work incremental theory of plasticity with isotropic hardening was used to determine the distribution of plastic strains of disks during loading.

Following the technique proposed, the calculations have been made on two aviation GTE disks (fig.1 and fig.2).

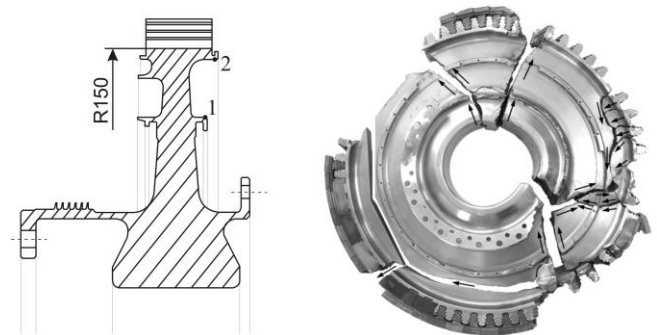


Fig.1. HPT disk № 1.  
Drawing and fragments of fractured disk (R in mm)

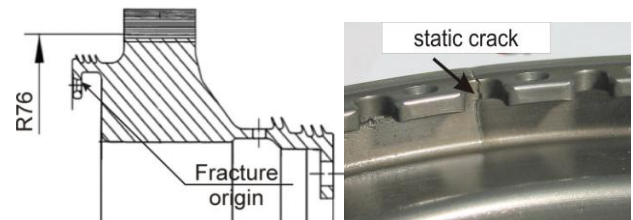


Fig.2. Power turbine disk № 2.  
Drawing and static crack of disk (R in mm)

The nickel powder alloy HPT disk №1 was loaded at normal temperature to the rotation rate  $n=0.96 \cdot n_{burst}$  and then stopped. Residual elongations have been measured for validation of material model parameters. After that disk №1 was brought to burst. Metallographic method showed that disk №2 originated its fracturing from the disk fir-tree slot bottom area. The power turbine disk №2 was made from new high-temperature forged Ni-based alloy; it was loaded at normal temperature up to the static macro crack initiation moment. Residual elongations and burst speed for experiment and quasi-static solutions are compared.

## 2. Tensile tests

With use of fracture criterion (3) to make calculative assessment of disk load-carrying capability, the  $U_*$  value is obtained at monotonic tensile tests (strain controlled conditions with standard strain rate according to ASTM E8/E8M-09 [6] and ASTM E21-09 [7]).

The tensile tests have been carried out at Schenck test machine (fig.3) which provides setting of maximum load up to  $P=100kN$ . This test machine contains precision frame, high-temperature clamps, hydraulic tooling. Specimen loading mode controlling and strain monitoring were performed using extensometer (25 mm base), installed on a working specimen part.

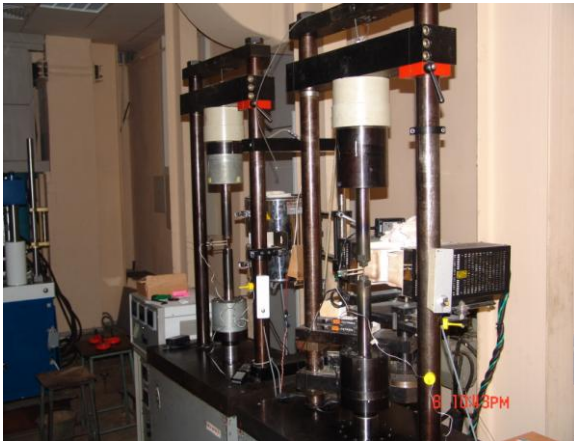


Fig.3. Schenck test machines

Tensile tests are carried out with getting full stress-strain curves up to ultimate stress followed by statistical processing of experimental data. The  $U_*(T)$  value in each test is defined as the area under stress-strain hardening curve at the given test temperature. For example, fig.4 shows full stress-strain diagram and definition of  $U_*$  for Ti-based and Ni-based alloys. Obviously, non-linear hardening law is necessary to use in material model.  $U_{*aver}$  and  $U_{*min}$  are the statistical average and minimal values derived of experimental data (black and red lines respectively).

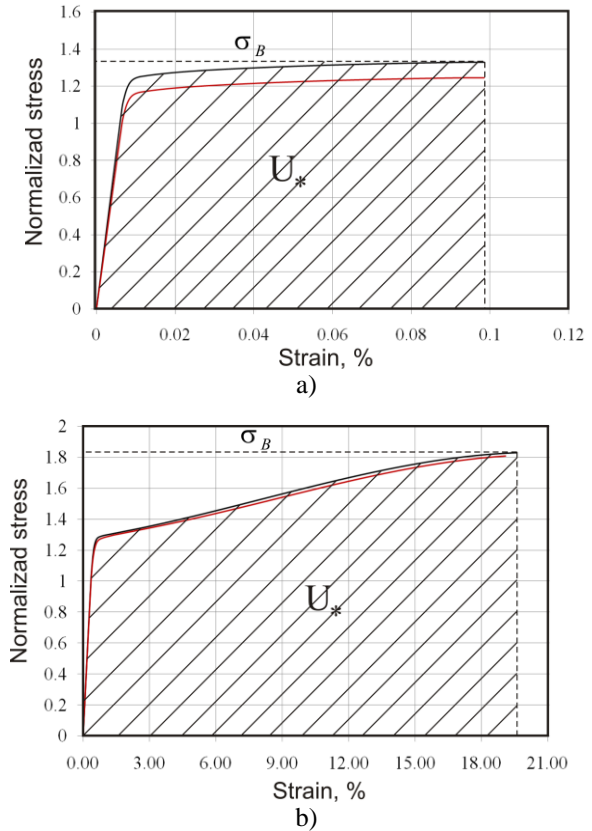


Fig.4. Definition of  $U_*$  (a-Ti based alloy, b-Ni based alloy)

## 3. Identification of material model parameters

During investigation load-carrying capability of turbo machine disks physical non-linearity should be taken into account. Physical non-linearity means occurrence of significant plastic strains in the process of loading (their value for materials of aircraft GTE disks exceeds 5%).

Incremental theory of plasticity with isotropic hardening was used to determine the distribution of plastic strains of disk during loading. The equivalent strain is split into elastic and plastic contributions. The increment of plastic strain is defined by the yield function:

$$\{d\varepsilon^{pl}\} = \lambda \left\{ \frac{\partial f}{\partial \sigma} \right\}, \quad (5)$$

where  $\lambda \geq 0$ . To define the best suited surface shape of the yield condition Hosford model is used in the yield function:

$$f = \sigma_{eqv} - \bar{\sigma}(\varepsilon) = 0, \quad (6)$$

$$\sigma_{eqv} = \left( \frac{(\sigma_1 - \sigma_2)^a + (\sigma_2 - \sigma_3)^a + (\sigma_3 - \sigma_1)^a}{2} \right)^{1/a}. \quad (7)$$

Yield loci  $(\sigma_1 - \sigma_2)^a + (\sigma_2 - \sigma_3)^a + (\sigma_3 - \sigma_1)^a = 2\sigma_{eqv}^a$  with several values of  $a$  is presented at fig.5. It is seen, that v.Mises criterion corresponds to  $a=2$  and the close to Tresca criterion to  $a \rightarrow \infty$ . Also, parameter  $a$  allows to describe surface between them.

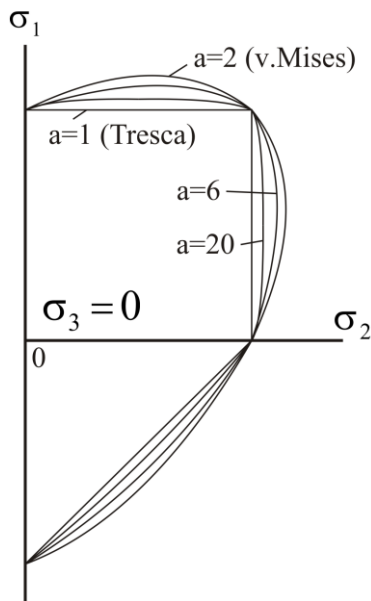


Fig.5. Yield loci of Hosford model with several values of  $a$

A non-linear hardening law  $\bar{\sigma}(\bar{\varepsilon})$  is obtained from full stress-strain diagram. The stress-strain curves of disk №1 alloy were obtained from tensile tests of 6 specimens cut out from disk work piece in circumferential direction. The stress-strain curves of disk №2 alloy were obtained from tensile tests of 6 specimens cut out from disk work piece in circumferential and radial directions.

The accuracy of parameter  $a$  have been validated by comparison of numerical  $\Delta_{exp} = \Delta R/R$  and experimental  $\Delta_{fem}$  residual deformations of disk №1 in points 1 and 2 (fig.1) and presented in table 1. Results with v.Mises criterion ( $a=2$ ) underestimate experimental results; results with close to Tresca criterion ( $a=80$ ) give good agreement with experimental residual elongations.

Table 1. Numerical and experimental residual deformations of disk №1 in points 1 and 2 (fig.1)

	Point 1	Point 2
$\Delta_{exp}, \%$	<b>0.78±0.04*</b>	<b>1.27±0.04*</b>
$\Delta_{fem}, \%$ ( $a=2$ )	0.060-0.068**	0.070-0.076**
$\Delta_{fem}, \%$ ( $a=20$ )	0.46-0.55**	0.55-0.65**
$\Delta_{fem}, \%$ ( $a=80$ )	1.00-1.19**	1.18-1.37**

\* - measurement error,

\*\* - material properties scattering.

The stress state of web disk №1 is mostly biaxial with high values of radial and circumferential stresses and limiting state becomes rapidly in case of Tresca criterion than v.Mises criterion. The calculations provided with Tresca yield condition had been found to be more reliable than v.Mises condition and used in calculations of burst speed. Also, it can be seen, that we had a big scattering (20%) in material properties using proposed material elastic-plastic model.

#### 4. Numerical simulation of burst speed

The technique is based on numerical simulation of spin tests using FEM wherein a disk is brought to burst. Simulation is performed in elastic-plastic statement specifying true stress-strain material curves and step-by-step increase in disk speed (quasi-static) until fracture energy density  $U_*$  reaches its critical value in most damaged disk point. Fig.6 and fig.7 illustrate examples of plotting finite-element grids for disks with detailed mesh in the zone of expected disk fracture.

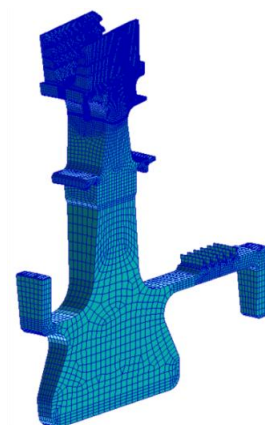


Fig.6. Finite-element grid of HPT disk №1

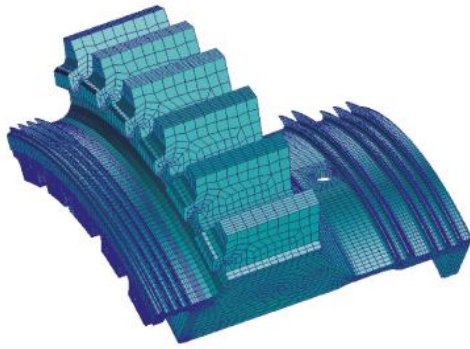


Fig.7. Finite-element grid of power turbine disk №2

Analysis of results of SSS calculations showed that the most damaged point (node with maximum values of  $\sigma_I$  and  $\sigma_{II}$ ) and the crack originating area coincided in experiments. At step-by-step disk loading all the components of strain and stress tensors grow monotonously.

Fig.8 illustrates for disk №1 changes of  $U_{aver}$  and  $U_{min}$  depending on the unit disk speed  $n/n_{100\%}$  calculated by average and the minimum values of mechanical properties. Prediction of burst speed with v.Mises criterion ( $a=2$ ) differ from experimental burst speed on 5-6%; with close to Tresca criterion ( $a=20...80$ ) calculation give accurate prediction (less than 1%) of burst speed. The traditional method (1) gives inaccurate prediction; the difference between calculation and experiment is 13%.

The burst speed value for disk №2 using the proposed material model with  $a=80$  and energy criterion differs from the experimental data by less than 2% (fig.9)

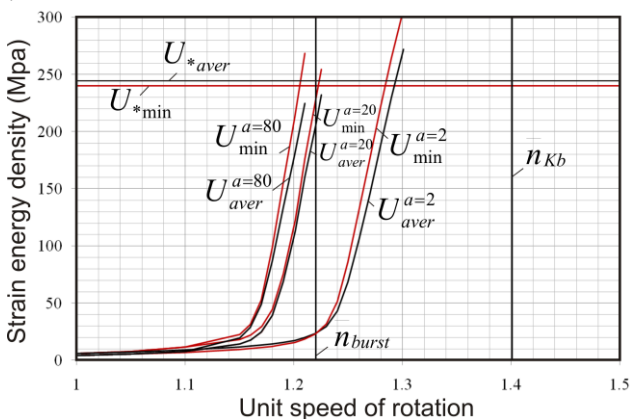


Fig. 8. Change of strain energy density in the most damaged disk № 1 point

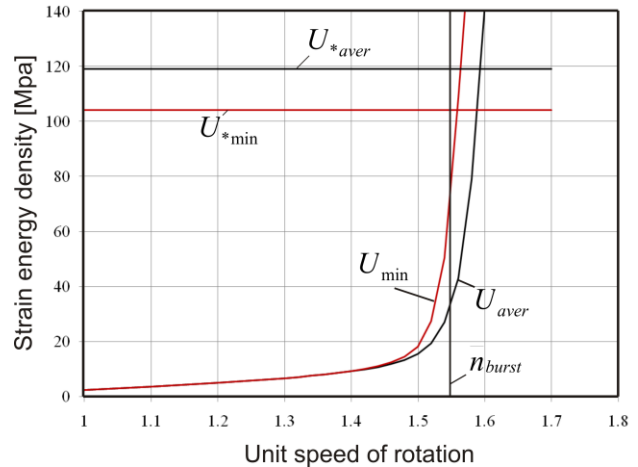


Fig. 9. Change of strain energy density in the most damaged disk № 2 point

### 5. Conclusion

Quasi-static FEM calculations of residual deformations and burst speed of two GTE disks was provided. For proposed elastic-plastic material model, Tresca yield condition has been found to be more reliable than v.Mises yield condition.

The energy fracture criterion has been proposed to be used to calculate a load-carrying capability of turbo machine disks. Possibility of this energy fracture criterion application has been verified. The burst speed calculations made for disks of different configurations and materials have shown satisfactory fit (less than 2%) to experimental data.

The technique developed for numerical determination of GTE disks burst speed will enable one not to carry out high-cost spin tests of disks. Numerical simulation involving the energy fracture criterion may be used to assess the load-carrying capability of disks taking into account the possible adverse combination of material properties and to optimize designs of rotors including the welded ones.

### Acknowledgement

The author acknowledges CIAM for permission to publish this work.

## References

- [1] Birger I.A., Shorr B.F., Demyanushko I.V., Sizova R.N., Dulnev R.A., Thermo strength of machine parts. // Moscow, "Mashinostroenie", 1975, 454 p.
- [2] Karimbaev K.D., Servetnik A.N. Numerical simulation of spin tests of turbo machine disks. // Engine building Herald, Scientific-technical journal, 2008, № 3, p. 130 – 134.
- [3] M. Maziere, et al., 2009. Overspeed burst of elastoviscoplastic rotating disks: Part I - Analytical and numerical stability analysis. European Journal of Mechanics A/Solids 28 36-44.
- [4] M. Maziere, et al., 2009. Overspeed burst of elastoviscoplastic rotating disks: Part II - Burst of a superalloy turbine disk. European Journal of Mechanics A/Solids 28 428-432.
- [5] Hosford W., 1972. A generalized isotropic yield criterion. J. Appl. Mech. 39, 607-609.
- [6] American Society of Test and Materials ASTM E8/E8M-09: standard test methods for tension testing of metallic materials, book of standards.
- [7] American Society of Test and Materials ASTM E21-09: standard test methods for elevated temperature tension tests of metallic materials, book of standards.

## Copyright Statement

The authors confirm that they, and/or their company or organization, hold copyright on all of the original material included in this paper. The authors also confirm that they have obtained permission, from the copyright holder of any third party material included in this paper, to publish it as part of their paper. The authors confirm that they give permission, or have obtained permission from the copyright holder of this paper, for the publication and distribution of this paper as part of the ICAS2012 proceedings or as individual off-prints from the proceedings.